Int. J. of GEOMATE, March, 2013, Vol. 4, No. 1 (Sl. No. 7), pp. 477-481
Geotec., Const. Mat. and Env., ISSN:2186-2982(P), 2186-2990(O), Japan

Lateral stress induced due root-water-uptake in unsaturated soils

Mu'azu Mohammed Abdullahi[1] and Nazri Bin Ali[1]
Faculty of Civil Engineering, Universiti Tecknologi Malaysia, Malaysia.

ABSTRACT: A two-dimensional (2-*D*) lateral stress was modeled as a result of matric suction change caused by vegetative induced moisture transfer. The negative pore-water pressures are estimated through governing partial differential equations for unsaturated soils. The results of the of simulated root water uptake are used as an input for the prediction of 2-*D* lateral stress in a stress-deformation analysis in an uncoupled manner. The soil is allow to expand and contract free laterally, as the as water is being abstracted from the soil. A mature Lime tree located on a Boulder clay sub-soil for period covering a full spring/summer drying period was used as a case study. The result shows interdependence of lateral and vertical stress generated resulting from root water-uptake.

Key words: Unsaturated soils, Numerical-simulation, Water-uptake, Stress-deformation, Experimental.

1. INTRODUCTION

When a material is compressed in one direction, it usually tends to expand in the other two directions perpendicular to the direction of compression,this phenomenon is known as the Poisson effect. The coefficient of lateral stress is a measure of the magnitude of the Poisson effect. In general soil mechanics, the deformation of soil matrix is analyzed as a result of increase in applied load, whereas in groundwater field, the soil deformation is studied due to extraction of groundwater. In both cases, a soil displacement takes place, because pore volume decreased [1]. Withdrawal of water by plant roots results in change in water pressures and moisture content in the soil. Soil settlement occurs whenever there is an increase in effective confining stress. In predictionof soil movement two fundamental stages are generallyinvolved; an assessment of the changes in moistureconditions and the knowledge of the volumetric strainsinduced by these change. A horizontal and vertical distribution of roots determines the dispersal of root water-uptake [1]-[2]

Thispaper employed two-dimensional axi-symmetrical finiteelement approach to solve the transient partial coupledflow and stress-deformation equations. The study wasbased on case study of mature single lime tree on aBoulder Clay as reported by [3], with the following objectives; to employtwo-dimensional axi-symmetrical finite elementapproach to solve the transient partial coupled flow and deformation equations and to simulate the water-uptakeand deformation. The capillary potentialwas estimate as a result of the root water-uptake waspartial coupled to estimate the lateral and vertical displacements as a resultof vegetative induced matric suction changes.

2. THEORETICAL FORMULATIONS SOIL MOISTURE MOVEMENT

The first step is dealt with through the use of modified Richard equation [4]; two-dimensional axi-symmetric governing equation for unsaturated soils with sinks term:

$$\frac{\partial \theta}{\partial \psi} \cdot \frac{\partial \psi}{\partial t} = \frac{\partial}{\partial z}\left[K(\psi)\frac{\partial \psi}{\partial z}\right] + \frac{1}{r}K\frac{\partial \psi}{\partial r} + \frac{\partial}{\partial r}\left[K(\psi)\frac{\partial \psi}{\partial r}\right] + \frac{\partial K(\psi)}{\partial z} - S(\psi, r, z) \qquad (1)$$

Where $K(\psi)$ is the unsaturated hydraulic conductivity, t is the time, r and z are the coordinate, θ is the volumetric moisture content and ψ is the capillary potential, $S(r, z)$ is the root water extraction function and r is the radial coordinate.

The root water-uptake extraction function is the sink term $S(\psi, z, r)$ in the Equation 1; for water-uptake in two-dimensional axi-symmetric form [5]. Comprising of vertical and radial components incorporating water stress function when soil moisture is limiting:

$$S(\psi, z, r) = \frac{4T}{z_r r_r}\alpha(\psi)\left[1 - \frac{z}{z_r}\right]\left[1 - \frac{r}{r_r}\right] \qquad (2)$$

Where $\alpha(\psi)$ (dimensionless) is a prescribed function of the capillary potential referred to as water-stress function.

The numerical solution of Equation 1 was achieved via the finite element spatial discretization procedure and a finite-difference time-stepping scheme adopting particular Galerkin weighted residual approach. The parabolic shape functions and eight-node isoperimetric elements are employed [6].

3 GROUND DISPLACEMENT THEORETICAL FORMULATION

The second step is tackled through stress-deformation formulation considering unsaturated soil mechanics concept using ground water field concept. Constitutive relationships are to compliment governing flow equation, thus, providing additional relationship between deformation and stress state variables. A change in the negative pore-water pressure occurs as a result of root water-uptake and can be related to changes in soil volume through the use of constitutive relations. Swelling in the field occurs along the rebound curve at an overburden pressure. Shrinkage occurs along either a recompression curve or the virgin compression curve. While the soil is a normally consolidated clay with a consolidation behavior that can be described by;

$$de = C_r \ln\left(\frac{\sigma_v + \Delta\sigma_v - u_{wf}}{(\sigma_v - u_a) + (u_a - u_w)_e}\right) \qquad (3)$$

Where deis the change of void ratio in the element, C_r is the re-compression index,σ_v is the vertical total stress, $\Delta\sigma_v$ is the change in the total vertical stresses, u_{wf} is the final pore water pressure, and $(u_a\text{-}u_w)_e$ is the matric suction equivalent [7].

4 DISCRETIZATION, BOUNDARY AND INITIAL CONDITIONS

The mesh consists of 8-noded isoperimetric linear strain quadrilateral elements. The entire finite element mesh consists of 1281 nodes and 400 elements; the axi-symmetric domain is shown in Figure 1. The mesh was configured to offer some refinement within the root zone area, since this is the region where the most significant moisture content variations were expected to occur.Spatial discretisation has been achieved via the finite element mesh shown in Figure 1.

The simulation employs a time-step size of 21600 seconds, which was held constant for the entire period considered. The lower boundary of the domain and the far-field vertical and horizontal boundaries remained unconstrained (natural) throughout the simulation. The soil parameters are shown in Table 1 for Boulder clay. Based on the field observations provided by [3], the root zone of matured Lime tree is assumed to extend to a depth of 2.0 m and a radial distance of 5.0

Where K_s*is* saturated hydraulic conductivity, T_a is actual transpiration rate, Ψ_w is suction at wilting point,γ is unit weight of soil, $e_0$is initial void ratio, $C_r$is re-compression index, μ is Poisson's ratio, $\theta_r$is residual water content, $\theta_s$is saturated water content, α is water stress, m is empirical shape fitting parameters, n is empirical shape fitting parameters and l is soil specific parameter generally assumed to be 0.5. The required soil moisture retention characteristics and unsaturated hydraulic conductivity was simulated from the closed form equation developed by [13].

5 CASE STUDY ON MATURE LIME TREE ON BOULDER CLAY

The particular experimental data is based on the field measurements undertaken at a site located at Stacey Hall, Wolverton, England [14]. The case considered here relates to a single mature Lime tree, 15 m in height, located on a Boulder clay sub-soil. A uniform initial value of capillary potential of -17 cm was applied throughout the domain; representing an initial volumetric water content of 37.5 % which corresponds to a degree of saturation of approximately 93.75 % was used as an initial value of capillary potential.The initial value of capillary potential would be in steady state and the subsequent steady state value is applied to the simulation. The drying phase was represented via the application of the transpiration rate.

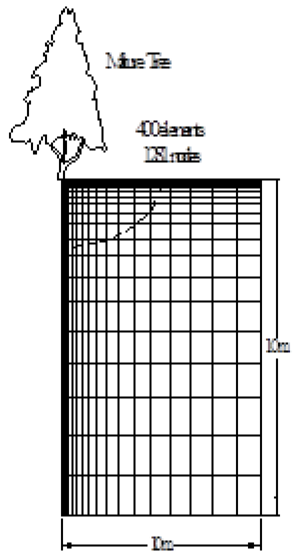

Fig. 1 Finite element mesh (10 m x 10 m)

Table 1 Parameters used in the analysis for Case I

Parameters	Values	References
k_s	10^{-6} m/s	[3]
T_a	5 mm/day	[3]
ψ_d	1500 kPa	[8]
γ	19.65 kN/m^3	[9]
e_0	1.25	[10]
C_r	0.023	[11]
μ	0.30	[12]
θ_r	0.1	[5]
θ_s	0.55	[5]
α	0.028	[5]
m	0.29	[5]
n	1.4	[5]
l	0.5	[5]

6 Results and Discussions

The graphs of variation of lateral and vertical ground displacement with depth at various lateral distances from Lime tree after 30 days are shown in Figs. 2 and 3. Lateral ground displacements are denoted with positive signs while the vertical ground displacements are denoted with negatives signs. The vertical displacements seem to be lager in magnitude than the lateral displacements. For 30 days simulation 7.13 mm vertical ground displacement at zero lateral distance from the Lime tree was achieved compared to zero lateral ground displacement at the same lateral away from the lime tree. The result shows that there is no lateral ground displacement beneath the Lime tree.

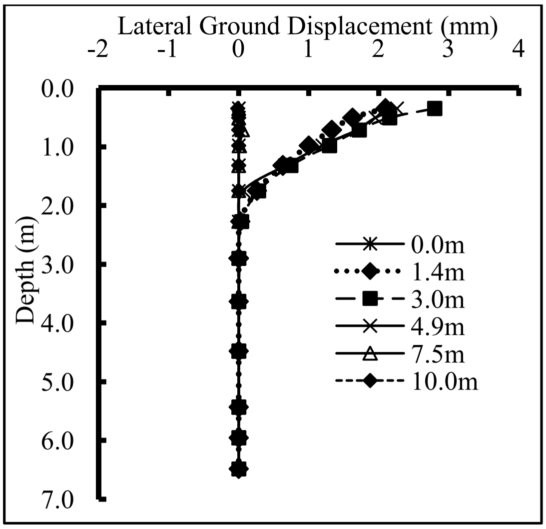

Fig. 2 Variation of lateral ground displacement with depth at various lateral distances from Lime tree after 30 days.

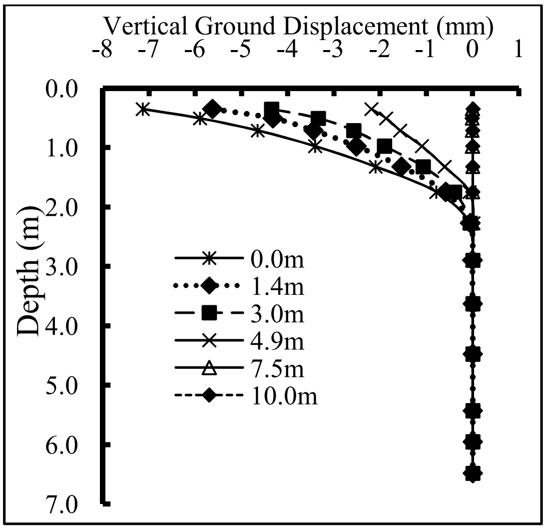

Fig. 3 Variation of vertical ground displacement with depth at various lateral distances from Lime tree after 30 days.

The variations of lateral and vertical ground displacement with depth at various lateral distances from Lime tree after 190 days are shown in Figs. 4 and 5. Fig. 4 show lateral ground displacement for 190 days simulation, a zero lateral displacement was recorded at zero lateral distance from the Lime tree. 18.67 mm, 19.34 mm and 6.76 mm lateral ground displacements at 1.4 m, 3.0 m and 4.9 m away from the lime tree respectively are simulated. At distance of 7.5 m and 10.0m away from Lime tree, -12.23 mm and -15.11 mm lateral ground displacements are simulated. This means at the distance of 7.5 m and 10.0 m away from the lime tree the effect of root water uptake is negligible. This shows that there is likely expansion instead of lateral shrinkage of the Boulder Clay.

The vertical ground displacements are shown in Fig. 5. Vertical ground displacements -79.16 mm, -48.70 mm, -29.64 mm and -6.58 mm at 0.0 m 1.4 m, 3.0 m and 4.9 m away from the lime tree respectively are shown in Fig. 5. At distance of 7.5 m and 10.0m away from Lime tree, 6.70 mm and 6.11 mm vertical ground displacements are simulated. Similarly, its means at the distance of 7.5 m and 10.0 m away from the lime tree the effect of root water uptake is negligible. This shows that there is likely heave instead of vertical ground displacement of the Boulder Clay.Lateral and vertical ground displacements with depth at various lateral distances from Lime tree after 270 days are shown in Figs. 6 and 7. The sequence is the same with Figs. 2, 3, 4 and 5, both vertical and lateral displacement increase with an increase in elapse time and decreases with depth. TheLateral and vertical ground displacements with depth at various lateral distances from Lime tree after 260 days are shown in Figs. 8 and 9 respectively.

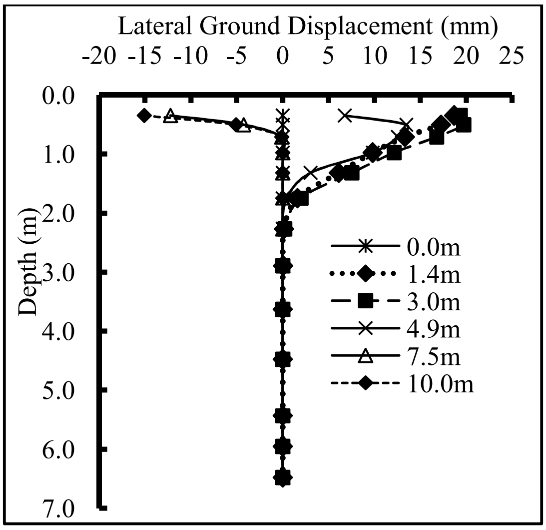

Fig. 4 Variation of lateral ground displacement with depth at various lateral distances from Lime tree after 190 days.

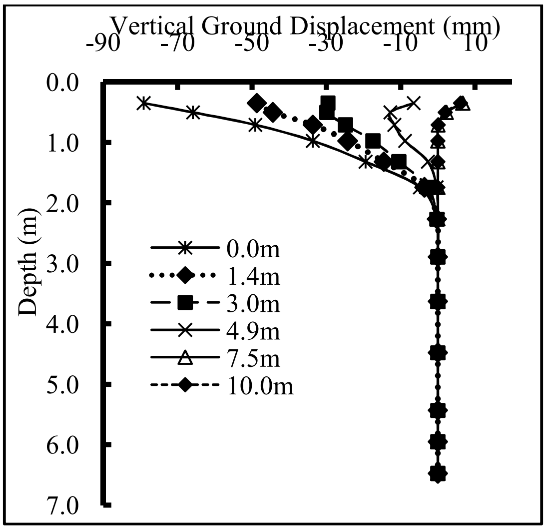

Fig. 5 Variation of vertical ground displacement with depth at various lateral distances from Lime tree after 190days.

The results shows general decrease in ground movement as the radial distance increase further away from the tree trunk as can be seen in Fig. 8 and 9 for 360 days. Meanwhile the magnitude of both lateral and vertical displacement increase with time. The effect of rainfall was included; rainfall data provided by the Bureau of Meteorology [14] has been acquired for the nearest weather station to the Wolverton Hampshire site. The results the simulated period that covers a spring/summer soil drying phase of 6 months followed by an autumn/winter 6 month recharge phase. The sink term was activated, to represent water uptake by transpiration, during spring/summer soil-drying phase and deactivated during the autumn/winter recharge phase. Therefore, the vertical and lateral displacements also followed that pattern.

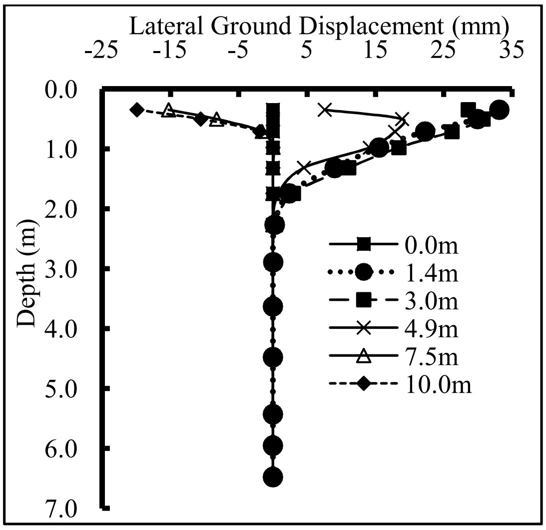

Fig. 6 Variation of lateral ground displacement with depth at various lateral distances from Lime tree after 270 days

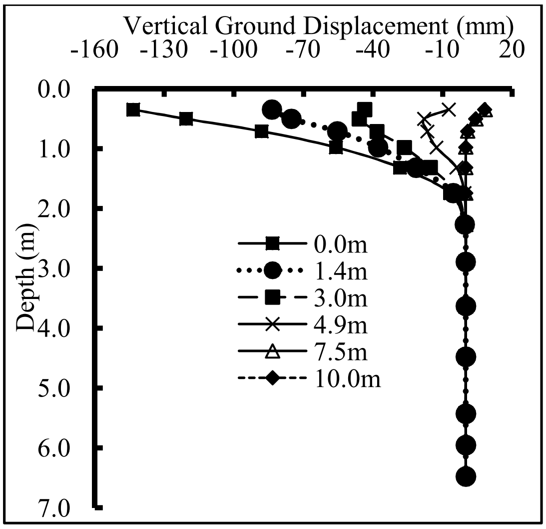

Fig. 7 Variation of vertical ground displacement with depth at various lateral distances from Lime tree after 270 days

7. CONCLUSIONS

The approach proposed utilizes radial symmetry and a linear distribution of water extraction rate with both depth and radius. The results of the root water-uptake analysis are then used as an input for the prediction of displacements in a stress-deformation analysis in an uncoupled manner. A mature Lime tree located on Boulder clay sub-soil covering a full spring/summer drying period was considered for the case study. The majority of the moisture extraction occurred near the surface; likewise, the ground displacement occurred mostly near the ground surface. Ground displacement reduced significantly when the distance from the tree increased. Both lateral and vertical displacements are time and space dependent. The accuracy of the lateral ground displacement simulation depends on accurate determination of the magnitude of the Poisson effect.

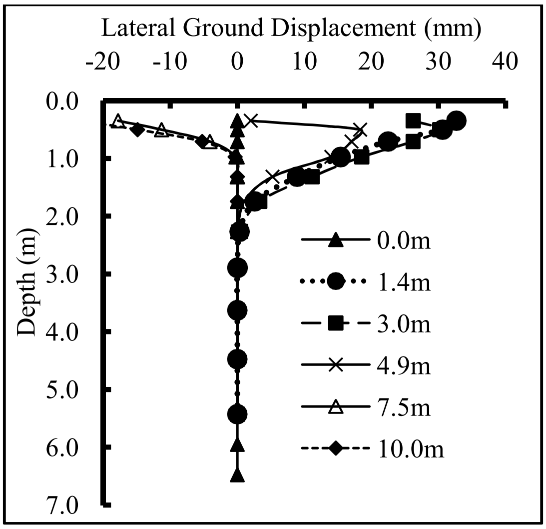

Fig. 8 Variation of lateral ground displacement with depth at various lateral distances from Lime tree after 360 days

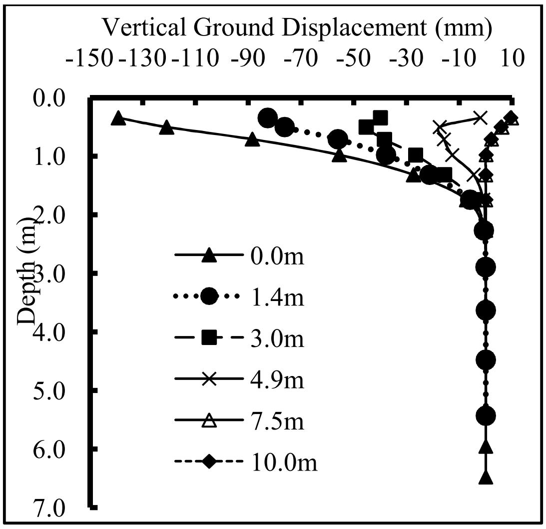

Fig. 9 Variation of vertical ground displacement with depth at various lateral distances from Lime tree after 360 days

8. REFERENCES

[1] Ali N, Mu'azu MA, Kamarudin A (2010). 2-D Axi-Symmetric of Root Water-Uptake. The

8thInternational Confereence on Geotechnical and Transportation Engineering, Sustainability in Geotechnical and Transportation Engineering, (GEOTROPIKA 2010) 1-3 December 2010. Kota kinabalu, Malaysia, pp. 1-5.

[2] Mu'azu MA, Ali N, Ahmed K (2010). Rainfall evaluation of root water-uptake induced deformation, ARPN Journal of Eng. and Applied Science, 5(8): 32-41.

[3] Biddle PG (1998). Tree Root Damage to Buildings, Pattern of soil Drying in Proximity to Trees on Clay Soils. 1st Edn., Vol. 2, Willow mead Publishing Ltd, Wantage, pp: 88-93.

[4] Richards LA (1931). Capillary conductance of liquids through porous mediums, Physics 1, pp. 318-333.

[5] Rees SW, Ali N (2006). Seasonal water uptake near trees: A numerical and experimental study. Geomechanics and Geo-Engineering, 1(2): 129-138.

[6] Zienkiewicz OC, Taylor RL (1989). The Finite Element Method. 4th Edn., Vol. 1, McGraw-Hill, USA., pp: 648.

[7] Fredlund DG, Rihardjo H (1993). Soil Mechanics for Unsaturated Soil. 1st Edn., John Wiley and Sons Inc., New York, pp: 346-373.

[8] Feddes RA, Kowalik PJ, Malink KK, Zaradny H (1976). Simulation of field water uptake by plants using a soil water dependent root extraction function. J. Hydro, 31: 13-26.

[9] Indraratna B, Fatahi B, Khabbaz H (2006). Numerical analysis of matric suction effects of tree roots." Geotechnical Engineering, 159(2):77 – 90.

[10] Samuels SG (1975). Some properties of the Gault Clay from Ely-Ouse Essex water tunnel, Geotechnique, 25(2): 239-264.

[11] Ng CWW (1998). Observed performance of multi-propped excavation in stiff clay, J. Geoenv., 124(9): 889-906.

[12] Almeida MSS, Britto AM, Perry RHG (1986). Numerical modeling of a centrifuged embankment on soft clay, Canadian Geotechnical Journal, 23(20): 103-114.

[13] vanGenuchten MT (1980). A closed-form equation for predicting the hydraulic conductivity of unsaturated soils. Soil Sci. Soc. Am. J., 44(5): 892-898.

[14] Bureau of Meteology (2006) United Kingdom Bureau of Meteology Meteorological Rainfall Data (1979-1980), Meteorological Office, Exeter, United Kingdom, 2006

Int. J. of GEOMATE, March, 2013, Vol. 4, No. 1 (Sl. No. 7), pp. 477-481.

MS No. 2165 received July 27, 2012, and reviewed under GEOMATE publication policies.

Pertinent discussion including authors' closure, if any, will be published in the March 2014 if the discussion is received by Sept, 2013.

Corresponding Author:Mu'azu Mohammed Abdullahi